




Xiang Liu · Lizhong Jiang · Ping Xiang  · Wangbao Zhou ·  
Zhipeng Lai · Yulin Feng

# Stochastic finite element method based on point estimate and Karhunen–Loève expansion

Received: 28 March 2020 / Accepted: 12 October 2020 / Published online: 4 January 2021  
© Springer-Verlag GmbH Germany, part of Springer Nature 2021

**Abstract** The present study proposes a new stochastic finite element method. The Karhunen–Loève expansion is utilized to discretize the stochastic field, while the point estimate method is applied for calculating the random response of the structure. Two illustrative examples, including finite element models with one-dimensional and two-dimensional stochastic fields, are investigated to demonstrate the accuracy and efficiency of the proposed method. Furthermore, two classical finite element analysis methods are used to validate the results. It is proved that the proposed method can model both the one-dimensional and the two-dimensional stochastic finite element problems accurately and efficiently.

**Keywords** Stochastic finite element method · Stochastic field · Karhunen–Loève expansion · Point estimate method

## 1 Introduction

The finite element method (FEM) is an efficient approach to analyze structural responses [1–4]. When considering some random properties, such as materials, geometry, and loads, the structural parameters can be set accordingly [5]. Numerous methods for random and reliability analysis with random variables have been proposed and applied in engineering, including the first-order reliability method (FORM), the second-order reliability method (SORM), Monte Carlo simulations (MCS) [6], the response surface method (RSM), and the point estimate method [7]. However, for all these methods, a major drawback is that spatial uncertainty variations in structural systems cannot be considered in the analysis. Thus, a more accurate approach to solve this

---

X. Liu · L. Jiang · P. Xiang (✉) · W. Zhou · Z. Lai  
School of Civil Engineering, Central South University, Changsha 410075, Hunan, China  
e-mail: pxiang2-c@my.cityu.edu.hk; pxiang@csu.edu.cn

X. Liu  
e-mail: liuxiang2017@csu.edu.cn

L. Jiang · P. Xiang · W. Zhou · Z. Lai  
National Engineering Laboratory for High-speed Railway Construction, Changsha, China

Y. Feng  
School of Civil Engineering and Architecture, East China Jiaotong University, Nanchang 330013, China

P. Xiang  
Jiangsu Key Laboratory of Environmental Impact and Structural Safety in Engineering, China University of Mining and Technology, Xuzhou, China

P. Xiang  
Engineering Research Center for Seismic Disaster Prevention and Engineering Geological Disaster Detection of Jiangxi Province, Nanchang, China

problem would consist in modeling parameters as spatial stochastic fields and adopting parameter stochastic fields into the response analysis [8, 9].

A computational approach combining FEM with the stochastic fields of the parameters has been implemented into the stochastic finite element method (SFEM) [10–13]. In previous work, a perturbation method was used for the SFEM (PSFEM) [14, 15]. Liu et al. [16, 17] applied PSFEM to solve static nonlinear problems and elastoplastic dynamics problems; Kleiber and Hien [10] published a monograph on PSFEM. Additionally, in the basic framework of PSFEM, other SFEMs were proposed: Shinozuka and Deodatis [18] combined high-order perturbation expansion and MCS using the Neumann expansion; Deodatis [19] combined PSFEM with the weighted integration method of stochastic fields and proposed a new concept for the mutation response function, which was applied to several SFEM problems [20]; Lei and Qiu [21, 22] used the Neumann SFEM to analyze dynamic problems. However, there are a few disadvantages associated with using PSFEM: The error is large when the coefficient of variation (COV) is large; furthermore, in dealing with static problems and dynamic time history problems, high-order terms contain duration items; thus, increasing the order does not improve the accuracy [11]. Ghanem and Spanos proposed the spectral stochastic finite element method (SSFEM) [11]. In this approach, the structural response is expanded through the orthogonal polynomial of the basic variables. If the structural basic variables follow the independent normal distribution, the weight function in the integral value of the response quantity expectation operator has a square exponential form. Ghanem and Spanos chose the polynomial chaos expansion (PCE) as the base for this expansion. SSFEM is the most widely used analytical method for SFEM. Füssl et al. [23] applied SSFEM to calculate the statistical moments of glued-laminated timber beams considering stochastic fields of interlayer stiffness. Slope reliability was analyzed through SSFEM in Ref. [24]. Wu and Law used SSFEM to deal with the vehicle–bridge dynamics considering the stochastic process of bridges and road roughness [25, 26]. Ghanem used this approach to solve the problem of transport in porous media [27], while further applications of SSFEM can be found in Refs. [28–30].

Several different methods exist for the discretization of stochastic fields, such as the midpoint method (MPM) [31], the average discretization method (ADM) [32], and the series expansion method (SEM), which itself includes the Karhunen–Loève expansion (KLE) [11], the orthogonal series expansion (OSE) [33, 34], and the expansion optimal linear estimation method (EOLE) [35]. Details about the accuracy and efficiency evaluation for each method can be found in Ref. [36]. In the present study, the Karhunen–Loève expansion was used.

The point estimate method (PEM) was first proposed by Rosenblueth [37]; the reliability analysis based on PEM does not require to solve functions derivatives and search the design point. Rather, this approach approximates the failure probability directly through the value of the function at several characteristic points. Subsequently, Seo et al. [38], Zhao and Ono [39], Zhou and Nowak [40], and Fan et al. [41] proposed a new and improved point estimate method. The essence of this new PEM consists of the Gaussian numerical integration. Multiple parameters are necessary for the expansion of the stochastic process using KLE, and it was proved that PEM can model a random system with multiple variables accurately and efficiently [41]. Furthermore, it was demonstrated that KLE–PEM can be applied to the train–track–bridge system efficiently [7, 42, 43]. In this paper, PEM is utilized to calculate the random response of SFEM.

This paper is organized as follows: Firstly, the KLE approach is introduced; secondly, the PEM approach based on the dimension reduction method is briefly introduced; a stochastic finite element method based on KLE and PEM is then proposed, and the equation for the random response of the one-dimensional and two-dimensional SFEM is derived; finally, two numerical examples are analyzed to validate the proposed method, and the results obtained via MCS and SSFEM are used for comparison.

## 2 The Karhunen–Loève expansion

Let  $u(x, \theta)$  be a stochastic process, which is a real-valued stochastic process defined on the probability space  $(\Omega, A, P)$  and bounded interval  $D$ . Let  $\bar{u}(x)$  be the mean value of the stochastic process, and  $C(x_1, x_2)$  be the covariance function, which is bounded, symmetric, and positive according to the definition of the autocovariance function. According to the Mercer's theorem, the covariance function can be expanded as:

$$C(x_1, x_2) = \sum_{i=1}^{\infty} \lambda_i f_i(x_1) f_i(x_2) \quad (1)$$

where the deterministic  $\lambda_i$  and  $f_i(x)$  are the eigenvalues and eigenfunctions of the covariance function  $C(x_1, x_2)$ , respectively. They can be obtained through the second Fredholm integral function, which can be written as:

$$\int_D C(x_1, x_2) f_i(x_1) dx = \lambda_i f_i(x_2) \tag{2}$$

where the eigenfunction  $f_i(x)$  satisfies the orthogonal property, which can be expressed as:

$$\int_D f_i(x_1) f_j(x_2) dx = \delta_{ij} \tag{3}$$

where  $\delta_{ij}$  is the Kronecker delta. The stochastic process  $u(x, \theta)$  can be expressed as:

$$u(x, \theta) = \bar{u}(x, \theta) + \sum_{i=1}^{\infty} \sqrt{\lambda_i} \xi_i(\theta) f_i(x) \tag{4}$$

Equation (4) represents the Karhunen–Loève expansion (KLE).  $\xi_i(\theta)$  is a group of uncorrected random variables, which is characterized by the following properties:

$$E[\xi_i(\theta)] = 0, E[\xi_i(\theta)\xi_j(\theta)] = \delta_{ij} \tag{5}$$

where  $E[\cdot]$  is the expectation.

If  $u(x, \theta)$  is a Gaussian stochastic process,  $\xi_i(\theta)$  is then a set of standard normal random variables.

For our purposes, the first  $M$  terms in Eq. (4) must be truncated, which results in:

$$u(x, \theta) = \bar{u}(x, \theta) + \sum_{i=1}^M \sqrt{\lambda_i} \xi_i(\theta) f_i(x) \tag{6}$$

The accuracy of the representation of the stochastic field depends on  $M$ . The prerequisite for using KLE is that Eq. (2) can be solved. For several special cases, Eq. (2) can be solved via analytical methods, while for all other cases it can be solved numerically [36].

### 3 The point estimate method

The stochastic processes discussed in this paper are of Gaussian nature, so that the random variables in the expansion formula obey the standard normal distribution. It is assumed that  $Y = g(X)$  is a continued random variable, with a probability density function  $p(x)$ ; thus, the expectation and variance of  $Y$  can be expressed as:

$$E[Y] = E[g(X)] = \int_{-\infty}^{\infty} g(X) p(x) dx \tag{7}$$

$$D[Y] = E[(Y - \mu)^2] = \int_{-\infty}^{\infty} [g(x) - \mu]^2 p(x) dx \tag{8}$$

where  $E[\cdot]$  and  $D[\cdot]$  are the expectation and variance, respectively, and  $\mu = E[Y]$ .

It can be inferred from Eq. (6) that multiple random variables are necessary in the representation of the stochastic process. Therefore, the dimension reduction method [44] can be used to simplify this problem. A  $n$ -dimensional variable function  $g(X)$  can be approximated by several  $s$ -dimensional variable functions  $g^s(X)$ , which can be written as:

$$g(X) \cong g^s(X) = \sum_{i=0}^s (-1)^i C_{n-s+i-1}^i \sum_{k_1 < \dots < k_{k-i}} y_{s-i} \tag{9}$$

with  $y_{s-i} = g(c_1, \dots, c_{k_1-1}, x_{k_1}, c_{k_1+1}, \dots, c_{k_{s-1}-1}, x_{k_{s-1}}, c_{k_{s-1}+1}, \dots, c_n)$ , where  $\mathbf{c}$  is the reference point  $\mathbf{c} = [c_1, c_2, \dots, c_n]$  and  $s < n$ .

**Table 1** Abscissas and weights for the Gaussian–Hermite quadrature with  $r = 3, 5,$  and  $7$

$R$	$X_{GH}$	$W_{GH}$
3	0	1.18164
	$\pm 1.22474$	0.295409
5	0	0.945309
	$\pm 0.958572$	0.393619
	$\pm 2.02018$	0.0199532
7	0	0.810265
	$\pm 0.816288$	0.425607
	$\pm 1.67355$	0.0545156
	$\pm 2.65196$	9.71781E-4

The function  $g(X)$  can be represented by a one-dimensional variable function when  $s = 1$ . In this case,  $g(X)$  then becomes:

$$g(\mathbf{X}) \cong g^1(\mathbf{X}) = \sum_{i=1}^n g_i(X_i) - (n - 1)g(c) \tag{10}$$

with  $g_i(X_i) = g(c_1, \dots, c_{i-1}, X_i, c_{i+1}, \dots, c_n)$ .

By substituting Eq. (10) into Eqs. (7) and (8), the expectation and variance of  $g(X)$  can be approximately expressed as:

$$E[Y] \cong \sum_{i=1}^n E[g_i(\mathbf{X}_i)] - (n - 1)g(c) \tag{11}$$

$$M_{z2} = D[Y] \cong \sum_{i=1}^n E\{[g_i(\mathbf{X}_i) - \mu]^2\} - (n - 1)[g(c) - \mu]^2 \tag{12}$$

where  $\mu = E[Y]$  and  $M_{z2}$  denotes the variance of  $Y$ .

According to Eq. (7), Eq. (8), and the theory of Gaussian integration,  $E[g_i(\mathbf{X}_i)]$  and  $E\{[g_i(\mathbf{X}_i) - \mu]^2\}$  in Eqs. (11) and (12) can be determined according to:

$$E[g_i(\mathbf{X}_i)] = \sum_{l=1}^r \frac{w_{GH,l}}{\sqrt{\pi}} g_i(\sqrt{2}x_{GH,l}) \tag{13}$$

$$E[(g(\mathbf{X}_i) - \mu)^2] = \sum_{l=1}^r \frac{w_{GH,l}}{\sqrt{\pi}} \left[ g_i(\sqrt{2}x_{GH,l}) - \mu \right]^2 \tag{14}$$

where  $r$  is the number of estimating points of the Gaussian–Hermite integration, while  $x_{GH,l}$  and  $w_{GH,l}$  are the abscissas and weights for the Gaussian–Hermite integration, respectively. The values of these parameters are listed in Table 1.

Similarly, the third and fourth central moments of  $g(X)$  can be obtained through:

$$M_{z3} \cong \sum_{i=1}^n E\{[g_i(\mathbf{X}_i) - \mu]^3\} - (n - 1)[g(c) - \mu]^3 \tag{15}$$

$$M_{z4} \cong \sum_{i=1}^n E\{[g_i(\mathbf{X}_i) - \mu]^4\} - (n - 1)[g(c) - \mu]^4 \tag{16}$$

where  $M_{z3}$  and  $M_{z4}$  are the third and fourth central moments, respectively.

The mean value, the standard deviation value (Std. D), the skewness coefficient, and the kurtosis coefficient of  $g(X)$  can be respectively expressed as:

$$\begin{cases} m_1 = \mu \\ m_2 = \sqrt{M_{z2}} \\ m_3 = M_{z3}/m_1^3 \\ m_4 = M_{z4}/m_1^4 \end{cases} \tag{17}$$

The corresponding probability density function (PDF) and cumulative distribution function (CDF) of the response can be fitted through several methods. In this paper, the cubic normal distribution transformation method [22] is applied to calculate the PDF of the response.

## 4 The stochastic finite element approach

### 4.1 KLE–PEM

In this paper, only the elastic structure is considered. The KLE introduced in Sect. 2 is used to represent the stochastic field expansion of the structures. For one-dimensional stochastic fields, taking an Euler beam with a stochastic field of Young's modulus as an example, it is assumed that Young's modulus is a Gaussian stochastic field  $E(x, \theta)$  and that its mean value and SD are  $\bar{E}(x)$  and  $\sigma_E$ , respectively. The stochastic field can be expressed as:

$$E(x, \theta) = \bar{E}(x) + \tilde{E}(x, \theta) \quad (18)$$

where

$$\tilde{E}(x, \theta) = \sum_{i=1}^{M_E} \xi_i(\theta) \sqrt{\lambda_i} f_i(x) \quad (19)$$

In Eq. (19),  $M_E$  denotes the number of terms in the truncated expression for the stochastic field, while  $\xi_i(\theta)$  is a set of standard normal random variables.

According to the theory of the FEM, the stiffness matrix of the element with stochastic field is:

$$\mathbf{K}^e = \int_l \mathbf{B}_e^T E(x, \theta) I \mathbf{B}_e dx = \bar{\mathbf{K}}^e + \tilde{\mathbf{K}}^e \quad (20)$$

where

$$\bar{\mathbf{K}}^e = \int \mathbf{B}_e^T \bar{E}(x) I \mathbf{B}_e dx \quad (21)$$

$$\tilde{\mathbf{K}}^e = \int_l \mathbf{B}_e^T \tilde{E}(x, \theta) I \mathbf{B}_e dx = \sum_{i=1}^{M_E} \xi_{i1} \tilde{\mathbf{K}}_i^e \quad (22)$$

$$\tilde{\mathbf{K}}_i^e = \int_l \mathbf{B}_e^T \sqrt{\lambda_{i1}} f_{i1}(x) I \mathbf{B}_e dx \quad (23)$$

Here,  $\mathbf{B}_e$  denotes the strain–displacement matrix,  $I$  represents the section moment of inertia, T denotes the transpose of the matrix, and  $l$  is the length of the element. Assembling all element matrices, the system matrix can be obtained as:

$$\mathbf{K} = \bar{\mathbf{K}} + \tilde{\mathbf{K}} \quad (24)$$

where

$$\bar{\mathbf{K}} = \sum \bar{\mathbf{K}}^e \quad (25)$$

$$\tilde{\mathbf{K}} = \sum_{i=1}^{M_E} \xi_{i1} \left( \sum \tilde{\mathbf{K}}_i^e \right) \quad (26)$$

According to the static mechanics formula  $\mathbf{F} = \mathbf{K}\mathbf{X}$ , one can write:

$$\mathbf{X} = \mathbf{K}^{-1} \mathbf{F} \quad (27)$$

where  $\mathbf{X}$  is the displacement vector and  $\mathbf{F}$  is the force vector.

According to what discussed in Sect. 3, all abscissas and weights of  $\xi_i$  can be obtained. Since  $\xi_i$  is a set of unrelated standard normal random variables, the Gaussian–Hermite quadrature is chosen for the calculation. Thus, substituting the corresponding value of each quadrature point into Eq. (20), one obtains:

$$\mathbf{K}_i^l = \bar{\mathbf{K}} + w(l) \sqrt{\lambda_i} \varphi_i(x) + \sum_{j=1, j \neq i}^{M_E} w_c \sqrt{\lambda_j} \varphi_j(x) \quad (28)$$

where  $w(l) = \sqrt{2}x_{GH,l}$  and  $l = 1, 2, \dots, N_g$ , with  $N_g$  the abscissas number. Furthermore,  $i$  denotes the  $i^{\text{th}}$  random variable and  $w_c$  represents the corresponding value in the reference point  $\mathbf{c}$ . When  $\mathbf{c} = [0, 0, \dots, 0]$ , Eq. (28) can be simplified as:

$$\mathbf{K}_i^l = \bar{\mathbf{K}} + w(l)\sqrt{\lambda_i}\varphi_i(x) \quad (29)$$

Substituting Eq. (29) into Eq. (27), one can obtain the corresponding response  $\mathbf{X}_i^l$ ; then, substituting all  $\mathbf{X}_i^l$  into Eqs. (11) and (12), one can determine the random response of the system.

For two-dimensional stochastic fields, taking the plane stress problem as an example, and assuming that the Young's modulus of the structure is a two-dimensional Gaussian stochastic field, with mean value and standard deviation  $\bar{E}(x, y)$  and  $\sigma_E$ , respectively, then the stochastic field can be expressed as:

$$E(x, y, \theta) = \bar{E}(x, y) + \tilde{E}(x, y, \theta) \quad (30)$$

where

$$\tilde{E}(x, y, \theta) = \sum_{i=1}^{M_E} \xi_i(\theta)\sqrt{\lambda_i}f_i(x, y). \quad (31)$$

In Eq. (31),  $M_E$  indicates the number of terms in the truncated expression for the stochastic field and  $\xi_i(\theta)$  is a group of standard normal random variables.

The element stiffness matrix can be obtained via the theory of the finite element method, which can be expressed as:

$$\mathbf{K}^e = \tilde{\mathbf{K}}^e + \tilde{\mathbf{K}}^e \quad (32)$$

where

$$\tilde{\mathbf{K}}^e = \int_{\Omega} h\mathbf{B}^T \bar{E}(x, y)\mathbf{D}\mathbf{B}d\Omega \quad (33)$$

$$\tilde{\mathbf{K}}^e = \int_{\Omega} h\mathbf{B}^T \tilde{E}(x, y)\mathbf{D}\mathbf{B}d\Omega. \quad (34)$$

Here,  $h$  is the unit thickness,  $\mathbf{B}$  is the strain matrix, T is the transpose of the matrix, and the matrix  $\mathbf{D}$  is given by:

$$\mathbf{D} = \frac{1}{1 - \mu^2} \begin{bmatrix} 1 & \mu & 0 \\ \mu & 1 & 0 \\ 0 & 0 & \frac{(1-\mu)}{2} \end{bmatrix} \quad (35)$$

where  $\mu$  is the Poisson's ratio. Assembling each element matrix to obtain the system stiffness matrix, the remaining steps are similar to those illustrated for the one-dimensional stochastic finite element method.

## 4.2 Monte Carlo simulations

MCS can also be considered a statistical simulation method as well as a statistical test method. The Monte Carlo method is a numerical simulation approach which considers the probability phenomenon as a research object. Specifically, this approach consists in estimating unknown quantities by their corresponding statistical value obtained via the sampling survey method. MCS are suitable for the simulation test of a discrete system. When the number of samples in a MCS is large enough, the result is close to the exact solution; therefore, the Monte Carlo method is often used as an exact solution to verify the accuracy of a newly proposed method.

For SFEM, taking the random field of material properties as an example, a large enough number of random field samples can be obtained according to Eq. (30). The corresponding stiffness matrix  $\mathbf{K}$  can then be determined by substituting each random field sample into the SFEM system. Thus, the corresponding structural response of each random field sample can then be calculated. Finally, the statistical moment of each random field sample is calculated according to the responses.

The few simple steps of the KLE–MCS approach are here summarized:

*Step 1* using a random sampling method to obtain a sample of a set of  $\xi$  which obey the standard normal distribution;

*Step 2* substituting the sample  $\xi$  into Eq. (24) to determine the system matrix and then obtain the corresponding response value using Eq. (27);

*Step 3* repeating step 1 and step 2, the mean value and standard deviation of the system response can be obtained using MATLAB standard statistical functions (“mean” and “std,” respectively).

### 4.3 SSFEM

Using the polynomial chaos expansion (PCE), any random variable  $u(\theta)$  can be expanded as:

$$u(\theta) = a_0\Gamma_0 + \sum_{i_1=1}^{\infty} a_{i_1}\Gamma_1(\xi_{i_1}(\theta)) + \sum_{i_1=1}^{\infty} \sum_{i_2=1}^{i_1} a_{i_1i_2}\Gamma_2(\xi_{i_1}(\theta), \xi_{i_2}(\theta)) + \sum_{i_1=1}^{\infty} \sum_{i_2=1}^{i_1} \sum_{i_3=1}^{i_2} a_{i_1i_2i_3}\Gamma_3(\xi_{i_1}(\theta), \xi_{i_2}(\theta), \xi_{i_3}(\theta)) + \dots \tag{36}$$

where  $a_{i_1i_2i_3}$  is the expansion coefficient and  $\Gamma_p(\cdot)$  is the  $P$ -order PCE with  $M$  standard normal random variables as independent variables. For convenience, Eq. (36) can be written in a more compact form:

$$u(\theta) = \sum_{i=0}^{\infty} b_i\Psi_i(\xi(\theta)) \tag{37}$$

where  $b_i$  and  $\Psi_i(\xi(\theta))$  have a one-to-one correspondence with  $a_{i_1i_2i_3}$  and  $\Gamma_p(\cdot)$ .  $\Psi_i(\xi(\theta))$  satisfies the following relationship:

$$\langle \Psi_i\Psi_j \rangle = \langle \Psi_i^2 \rangle \delta_{ij} \tag{38}$$

where  $\delta_{ij}$  is the Kronecker delta. The symbol  $\langle \cdot \rangle$  denotes the inner product, and the value of  $\langle \Psi_i^2 \rangle$  can be calculated analytically [11].

In SSFEM, taking once more the elastic modulus as an example, the stochastic field of  $E(x, \theta)$  can be expanded via KLE and the response can be expanded using PCE, with the respective truncation terms being  $k_E$  and  $k_R$ . By substituting Eqs. (24) and (37) into Eq. (27), taking the inner product on both sides of the resulting equation with  $\Psi_k(\theta)$ , and employing the orthogonal property in Eq. (38), one obtains:

$$\sum_{j=0}^{k_R} \sum_{i=0}^{k_E} \langle \xi_i(\theta)\Psi_j(\theta)\Psi_k(\theta) \rangle \mathbf{K}_i u^{(j)} = \mathbf{f} \tag{39}$$

where  $\mathbf{K}_{k,j} = \sum_{i=0}^{k_E} \frac{\langle \xi_i(\theta)\Psi_j(\theta)\Psi_k(\theta) \rangle}{\langle \Psi_k^2 \rangle} \mathbf{K}_i$ . Equation (39) can be written in matrix form as:

$$\begin{bmatrix} \mathbf{K}_{0,0} & \mathbf{K}_{1,0} & \dots & \mathbf{K}_{K_R,0} \\ \mathbf{K}_{0,1} & \mathbf{K}_{1,1} & & \vdots \\ \vdots & & & \\ \mathbf{K}_{0,K_R} & \dots & & \mathbf{K}_{K_R,K_R} \end{bmatrix} \cdot \begin{Bmatrix} \mathbf{u}_0 \\ \mathbf{u}_0 \\ \vdots \\ \mathbf{u}_{K_R} \end{Bmatrix} = \begin{Bmatrix} \mathbf{f}_0 \\ \mathbf{f}_1 \\ \vdots \\ \mathbf{f}_{K_R} \end{Bmatrix} \tag{40}$$

and the response statistics can be evaluated as:

$$MEAN_{\mathbf{R}}(t) = \mathbf{y}^{(0)}(t), \quad VAR_{\mathbf{R}}(t) = \sum_{j=1}^{K_R} \left( \mathbf{y}^{(j)}(t) \right)^2 \langle \Psi_j^2 \rangle. \tag{41}$$

In these equations, the values of the inner product of PCE, denoted as  $\langle \cdot \rangle$ , are constants and they can be obtained analytically [11].

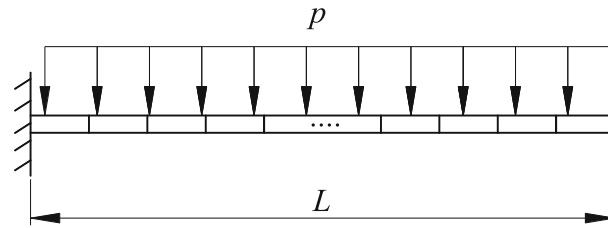


**Fig. 1** Beam with one-dimensional stochastic field

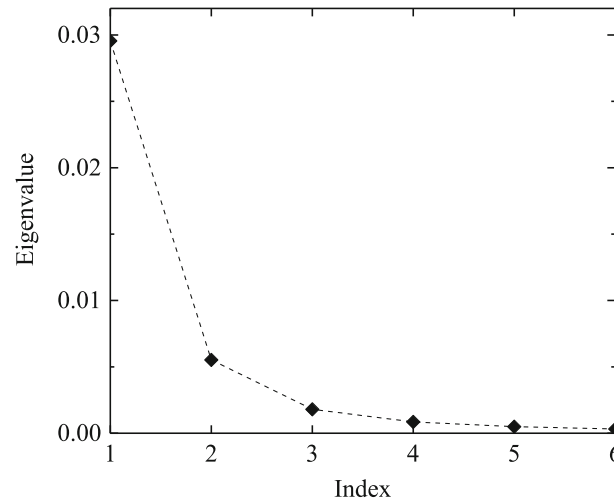


**Fig. 2** Eigenvalues realization of the stochastic field expansion

## 5 Numerical examples

### 5.1 Case 1: one-dimensional expansion

A cantilever beam, which is considered as a Euler–Bernoulli beam, is shown in **Fig. 1**. The length of the beam is 1; the beam is subjected to a specific uniform load  $p = 1$ . The bending rigidity  $w(x) \equiv EI$  of the beam, which includes the Young’s modulus  $E$  and the sectional moment inertia  $I$ , is a Gaussian stochastic process, indexed over the spatial domain occupied by the beam. The mean value  $\bar{w}(x)$  equals 1, and the covariance function  $C(x_1, x_2)$  of  $w(x)$  is:

$$C(x_1, x_2) = \sigma_E e^{-(|x_1 - x_2|/a)} \quad (42)$$

where  $\sigma_E$  is the standard deviation of  $w(x)$ ,  $a$  is the correlation length (which amounts to 1), and  $x_1$  and  $x_2$  take values within the range from 0 to 1.

The beam contains 10 elements. This example can be found in Ref. [11]. According to Sect. 4, a SFEM model based on the KLE–PEM approach was established and the eigenvalues trend of the stochastic field expansion is shown in **Fig. 2**. It can be seen that a KLE truncated at the fourth term is sufficiently accurate for the stochastic field representation.

**Figure 3** illustrates the KLE eigenfunctions. The numbers of abscissas  $r = 3, 5,$  and  $7$  are considered for calculation, thus requiring 9, 17, and 25 times for the calculation of SFEM models, respectively. The SFEM models based on MCS and SSFEM were established for comparison. **Figures 4** and **5** show the mean value and standard deviation value (Std. D) response, respectively, of each node of SFEM, when the coefficient of variation (COV) of  $w(x)$  equals 0.2. It can be seen from **Fig. 4** that the mean value of the response calculated via KLE–PEM is very close to the results calculated via MCS, which requires 5000 times calculation. Thus, using three estimated points only can provide the same results as using five and seven estimated points, with a maximum error of 0.1%. The SSFEM approach also has a higher accuracy. **Figure 5** illustrates the standard deviation of the vertical displacement response calculated via MCS, KLE–PEM, and SSFEM. By comparing with the other two methods, it can be found that the results obtained via KLE–PEM have a high precision,



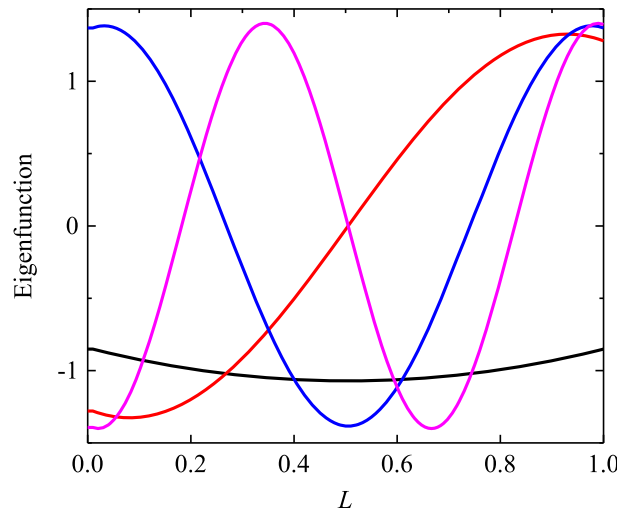


Fig. 3 Eigenfunctions for the four terms of the stochastic field expansion

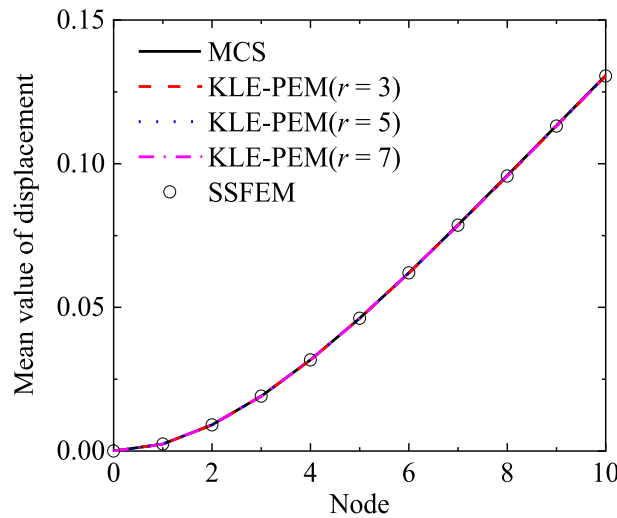


Fig. 4 Mean value of vertical displacement response for each node

Table 2 Time duration of each approach for SFEM

	MCS	KLE-PEM-3	KLE-PEM-5	KLE-PEM-7	SSFEM
Time for case 1 (s)	432.11	0.71	1.58	2.31	16.79
Time for case 2 (s)	485.94	1.31	2.57	3.86	26.54

The CPU was Inter(R) Core(TM) i7-7700 and the RAM was 16G

only slightly lower than that of SSFEM. By contrast, the computational efficiency of KLE-PEM is higher than SSFEM, and according to the calculation time data (see Table 2), KLE-PEM requires less calculation time than SSFEM under different integration points. The results obtained by using three, five, and seven estimate points are very close.

The first four moments of the SFEM response can be obtained through the KLE-PEM approach, and the PDF can be obtained using the cubic normal distribution transformation method [45], and then the corresponding cumulative distribution function (CDF) can be obtained. Figure 6 shows the comparison of plots for the CDF of the tip displacement calculated via KLE-PEM, SSFEM, and MCS. The CDF results calculated via the KLE-MCS can be obtained through the “ksdensity” command in MATLAB® software. An inspection of Fig. 6 reveals a very close agreement between the proposed method and MCS.

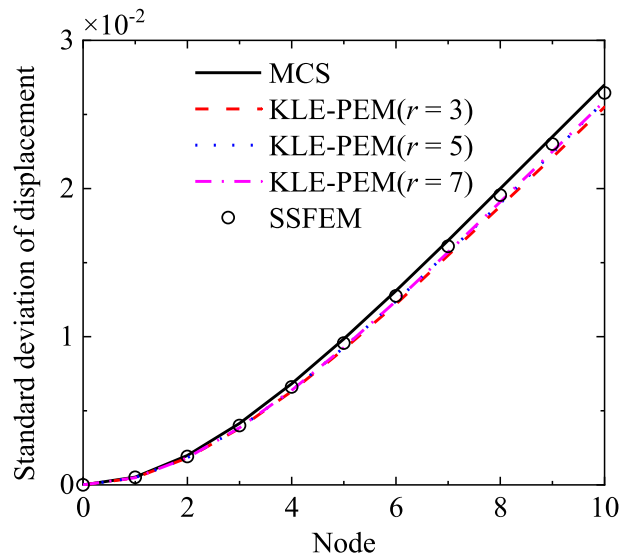


**Fig. 5** Standard deviation of vertical displacement response for each node

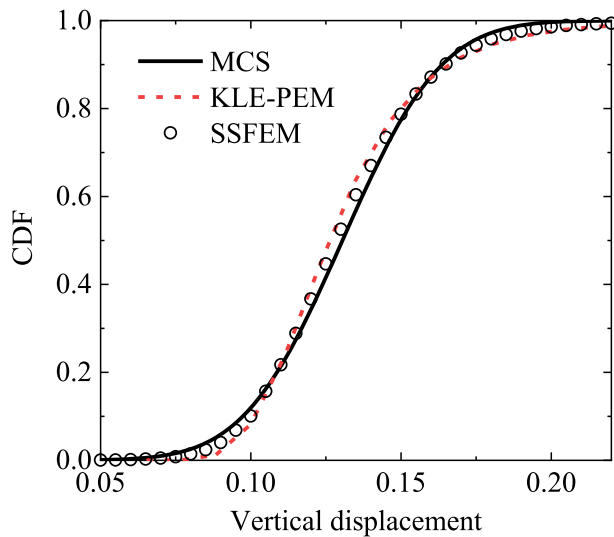


**Fig. 6** Cumulative distribution function of the tip displacement

Figures 7 and 8 show the mean value and the standard deviation of the tip displacement calculated via KLE-PEM with  $r = 3$ , while SSFEM and MCS were performed under different COVs. It can be seen that when the COV ranges between 0.10 and 0.25, the mean value and standard deviation value increase with the increase in COV. In addition, the calculation error of the KLE-PEM approach also increases. The KLE-PEM method is two to three orders of magnitude more efficient than MCS and one order of magnitude more efficient than SSFEM. The KLE-PEM approach has great advantages and can be used to analyze the reliability of the structure.

## 5.2 Case 2: two-dimensional expansion

In order to verify the applicability of the KLE-PEM approach in the two-dimensional stochastic field finite element method, a plane stress model was established, as shown in Fig. 9. This plane stress model has dimensions of  $L_x = 1.0$  m and  $L_y = 1.0$  m, with a thickness  $h = 0.05$  m. A total of 16 units are evenly divided, and a uniform load  $p = 1$  N/m<sup>2</sup> acts above the plane. It is assumed that the elastic modulus of the plane is a

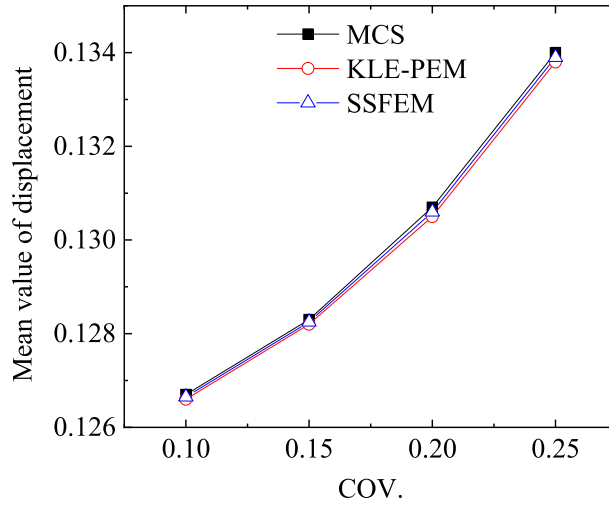


Fig. 7 Mean value of the tip displacement under different COVs

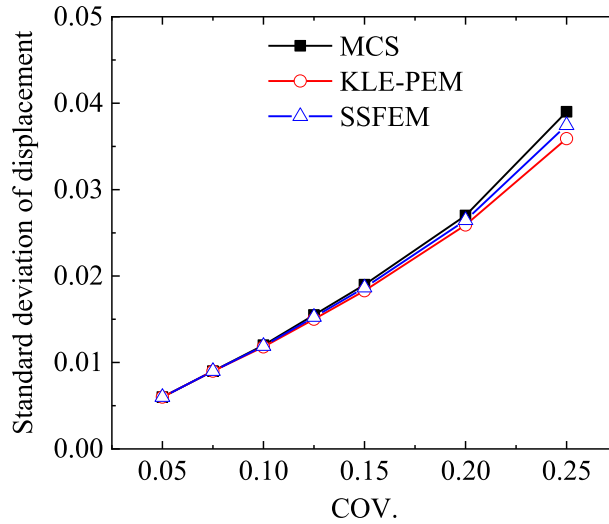


Fig. 8 Standard deviation of the tip displacement under different COVs

two-dimensional stochastic field  $E(x, y, \theta)$ , with a mean value  $\bar{E}(x, y, \theta) = 100$  Pa; the covariance function  $C(x_1, x_2; y_1, y_2)$  of  $E(x, y, \theta)$  is given by:

$$C(x_1, x_2; y_1, y_2) = \sigma_E e^{-|x_1 - y_1|/b_1 - |x_2 - y_2|/b_2} \tag{43}$$

where  $\sigma_E$  is the standard deviation of  $E(x, y, \theta)$ ,  $b_1$  and  $b_2$  are the correlation lengths, which are equal to  $L_x$  and  $L_y$ , respectively, the variables  $x_1, x_2, y_1$ , and  $y_2$  have a range from 0 to 1. A two-dimensional SFEM model was established in accordance with Sect. 4. Similarly, three, five, and seven estimated points were successively chosen to calculate the random response, and the different COVs of  $E(x, y, \theta)$  were determined separately. The results were compared with those obtained via MCS and SSFEM. A KLE truncated at the sixth term was found to be sufficiently accurate for the stochastic field representation here.

The response comparison between the three methods for the top and middle part of the plane, i.e., the vertical displacement of node “A” in Fig. 9, is shown in Figs. 10 and 11. It can be found from Fig. 10 that, when COV is in the range from 0.10 to 0.20, the mean value of the response increases with the increase in COV, and that the error of the KLE–PEM approach also increases. In addition, the mean value obtained through the three, five, and seven estimated points does not show a significant variation. It can be found in Fig. 11 that the standard deviation of the response increases with the increase in COV and that the error also increases substantially, in particular when COV exceeds 0.15. Furthermore, the error associated with using five and seven estimated

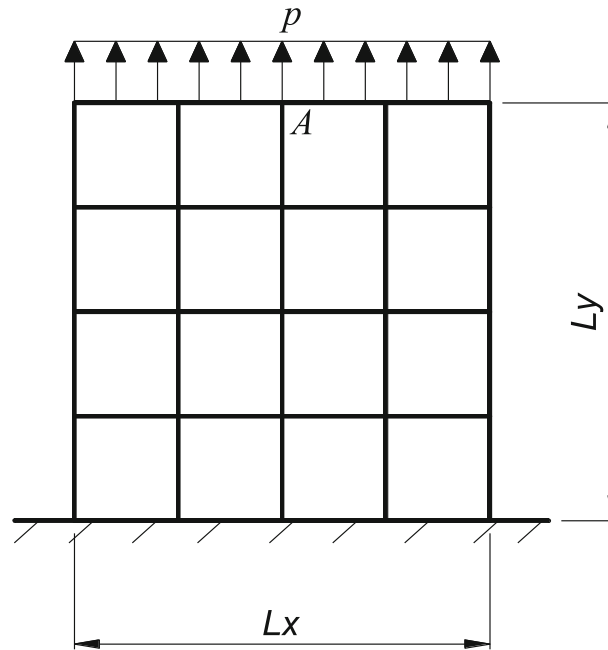


**Fig. 9** Plane stress model

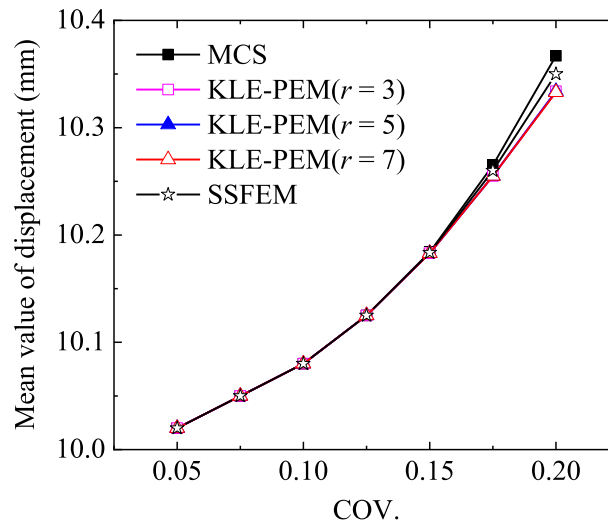


**Fig. 10** Mean value of plane top displacement under different COVs

points is slightly lower than when using three estimated points. When COV is 0.1, 0.15, and 0.2, the error of the standard deviation obtained via KLE-PEM with  $r = 5$  is 0.66%, 2.1%, and 5.3%, respectively. When COV is less than 0.125, the accuracy of KLE-PEM is not much different from that of SSFEM. By contrast, when COV is greater than 0.125, KLE-PEM performs less well than SSFEM. However, the computational efficiency of KLE-PEM is much higher than that of SSFEM (see Table 2). Therefore, KLE-PEM still has several advantages and numerous potential applications.

## 6 Conclusions

In this paper, a method for analyzing the random structure response with spatial parameter was proposed. The Karhunen-Loève expansion was used to represent the stochastic process of the spatial parameter, while the finite element theory was used to establish the structure model. The detailed parameter values of the structure

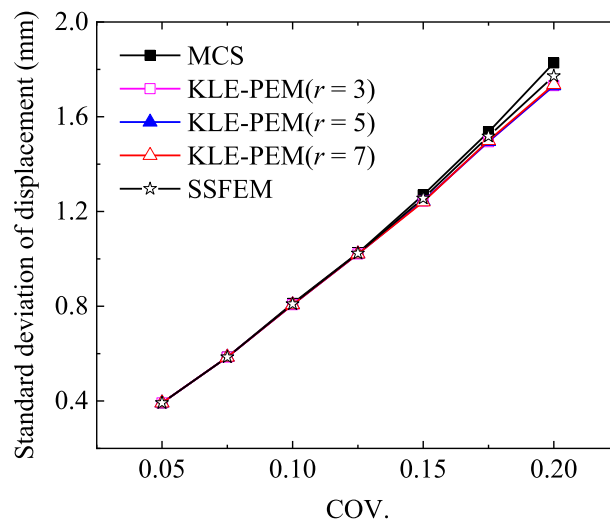


**Fig. 11** Standard deviation of plane top displacement under different COVs

were chosen according to the representation of the stochastic process. The point estimate method, which is based on the Gaussian integration and the dimensional reduction method, was adopted to calculate the random response of the structures. Two different types of finite element model examples were discussed, and certain conclusions could be drawn:

1. SFEM based on the KLE–PEM approach can model both the one-dimensional and the two-dimensional stochastic finite element method problems.
2. SFEM based on the KLE–PEM approach has a great accuracy and efficiency, and the efficiency of KLE–PEM is two to three orders of magnitude higher than that of MCS, and one order of magnitude higher than that of SSFEM.
3. The error of SFEM based on the KLE–PEM approach increases when the COV is larger than 0.175; despite this limitation, the proposed method is extremely efficient and thus it is proposed that this method is well suited in the case of a small coefficient of variation ( $\text{COV} \leq 0.175$ ).

**Acknowledgements** The work described in this paper is supported by grants from the National Natural Science Foundation of China (Grant Nos. U1934207, 51778630, and 11972379), the Fundamental Research Funds for the Central Universities of Central South University (Grant No. 2020zzts148), Jiangsu Key Laboratory of Environmental Impact and Structural Safety in Engineering, China University of Mining & Technology and Engineering Research Center for Seismic Disaster Prevention and Engineering Geological Disaster Detection of Jiangxi Province (SDGD202001).

#### Compliance with ethical standards

**Conflict of interest** The authors declare that they have no conflict of interest.

#### References

1. Pask, J.E., Sukumar, N.: Partition of unity finite element method for quantum mechanical materials calculations. *Extreme Mech. Lett.* **11**, 8–17 (2017). <https://doi.org/10.1016/j.eml.2016.11.003>
2. Zhang, T.: Deriving a lattice model for neo-Hookean solids from finite element methods. *Extreme Mech. Lett.* **26**, 40–45 (2019). <https://doi.org/10.1016/j.eml.2018.11.007>
3. Schroder, J., Wriggers, P., Balzani, D.: A new Mixed Finite Element based on Different Approximations of the Minors of Deformation Tensors. *Comput. Methods Appl. Mech. Eng.* **200**, 3583–3600 (2011). <https://doi.org/10.1016/j.cma.2011.08.009>
4. Schröder, J., Viebahn, N., Wriggers, P., Auricchio, F., Steeger, K.: On the stability analysis of hyperelastic boundary value problems using three- and two-field mixed finite element formulations. *Comput. Mech.* **60**, 479–492 (2017).

5. Schröder, J., Balzani, D., Brands, D.: Approximation of random microstructures by periodic statistically similar representative volume elements based on lineal-path functions. *Arch. Appl. Mech.* **81**, 975–997 (2011). <https://doi.org/10.1007/s00419-010-0462-3>
6. Sudret, B., Armen, D.K.: Stochastic finite element methods and reliability- A state of the art report
7. Jiang, L., Liu, X., Xiang, P., Zhou, W.: Train-bridge system dynamics analysis with uncertain parameters based on new point estimate method. *Eng. Struct.* **199**, 109454 (2019). <https://doi.org/10.1016/j.engstruct.2019.109454>
8. Batou, A., Soize, C.: Stochastic modeling and identification of an uncertain computational dynamical model with random fields properties and model uncertainties. *Arch. Appl. Mech.* **83**, 831–848 (2013). <https://doi.org/10.1007/s00419-012-0720-7>
9. Shen, L., Ostoja-Starzewski, M., Porcu, E.: Bernoulli-Euler beams with random field properties under random field loads: fractal and Hurst effects. *Arch. Appl. Mech.* **84**, 1595–1626 (2014). <https://doi.org/10.1007/s00419-014-0904-4>
10. Kleiber, M., Hien, T.D.: The stochastic finite element method: basic perturbation technique and computer implementation. Wiley, New York (1992)
11. Ghanem, R.G., Spanos, P.D.: Stochastic finite elements: A spectral approach. Dover Publications, New York (2003)
12. Vanmarcke, E.H., Shinozuka, M., Nakagiri, S., Schueller, G.I., Grigoriu, M.: Random fields and stochastic finite elements. *Struct. Saf.* **3**, 143–166 (1986). [https://doi.org/10.1016/0167-4730\(86\)90002-0](https://doi.org/10.1016/0167-4730(86)90002-0)
13. Mohammadi, J.: Reliability Assessment Using Stochastic Finite Element Analysis. *J. Struct. Eng.-Asce.* **127**, 976–977 (2001). [https://doi.org/10.1061/\(ASCE\)0733-9445\(2001\)127:8\(976.2\)](https://doi.org/10.1061/(ASCE)0733-9445(2001)127:8(976.2))
14. Liu, C., Wang, T.-L., Qin, Q.: Study on sensitivity of modal parameters for suspension bridges. *Struct. Eng. Mech.* **8**, 453–464 (1999) <https://doi.org/10.12989/sem.1999.8.5.453>
15. Zhang, Y., Chen, S., Liu, Q., Liu, T.: Stochastic perturbation finite elements. *Comput. Struct.* **59**, 425–429 (1996). [https://doi.org/10.1016/0045-7949\(95\)00267-7](https://doi.org/10.1016/0045-7949(95)00267-7)
16. Liu, W.K., Mani, A., Belytschko, T.: Finite element methods in probabilistic mechanics. *Probabilistic Eng. Mech.* **2**, 201–213 (1987). [https://doi.org/10.1016/0266-8920\(87\)90010-5](https://doi.org/10.1016/0266-8920(87)90010-5)
17. Liu, W.K., Belytschko, T., Mani, A.: Probabilistic finite elements for nonlinear structural dynamics. *Comput. Methods Appl. Mech. Eng.* **56**, 61–81 (1986). [https://doi.org/10.1016/0045-7825\(86\)90136-2](https://doi.org/10.1016/0045-7825(86)90136-2)
18. Shinozuka, M., Deodatis, G.: Response Variability of Stochastic Finite Element Systems. *J. Eng. Mech.-Asce.* **114**, 499–519 (1988). [https://doi.org/10.1061/\(ASCE\)0733-9399\(1988\)114:3\(499\)](https://doi.org/10.1061/(ASCE)0733-9399(1988)114:3(499))
19. Deodatis, G., Graham, L.: The weighted integral method and the variability response function as part of a SFEM formulation. In: Uncertainty modeling in finite element, fatigue and stability of systems. pp. 71–116. World Scientific (1997)
20. Graham, L., Deodatis, G.: Response and eigenvalue analysis of stochastic finite element systems with multiple correlated material and geometric properties. *Probabilistic Eng. Mech.* **16**, 11–29 (2001). [https://doi.org/10.1016/S0266-8920\(00\)00003-5](https://doi.org/10.1016/S0266-8920(00)00003-5)
21. Lei, Z., Qiu, C.: Neumann dynamic stochastic finite element method of vibration for structures with stochastic parameters to random excitation. *Comput. Struct.* **77**, 651–657 (2000). [https://doi.org/10.1016/S0045-7949\(00\)00019-5](https://doi.org/10.1016/S0045-7949(00)00019-5)
22. Lei, Z., Qiu, C.: A stochastic variational formulation for nonlinear dynamic analysis of structure. *Comput. Methods Appl. Mech. Eng.* **190**, 597–608 (2000). [https://doi.org/10.1016/S0045-7825\(99\)00431-4](https://doi.org/10.1016/S0045-7825(99)00431-4)
23. Füssl, J., Kandler, G., Eberhardsteiner, J.: Application of stochastic finite element approaches to wood-based products. *Arch. Appl. Mech.* **86**, 89–110 (2016). <https://doi.org/10.1007/s00419-015-1112-6>
24. Jiang, S.-H., Li, D.-Q., Zhang, L.-M., Zhou, C.-B.: Slope reliability analysis considering spatially variable shear strength parameters using a non-intrusive stochastic finite element method. *Eng. Geol.* **168**, 120–128 (2014). <https://doi.org/10.1016/j.enggeo.2013.11.006>
25. Wu, S.Q., Law, S.S.: Dynamic analysis of bridge with non-Gaussian uncertainties under a moving vehicle. *Probabilistic Eng. Mech.* **26**, 281–293 (2011). <https://doi.org/10.1016/j.probengmech.2010.08.004>
26. Wu, S.Q., Law, S.S.: Dynamic analysis of bridge-vehicle system with uncertainties based on the finite element model. *Probabilistic Eng. Mech.* **25**, 425–432 (2010). <https://doi.org/10.1016/j.probengmech.2010.05.004>
27. Ghanem, R.: Stochastic finite elements with multiple random non-Gaussian properties. *J. Eng. Mech.-Asce.* **125**, 26–40 (1999). [https://doi.org/10.1061/\(ASCE\)0733-9399\(1999\)125:1\(26\)](https://doi.org/10.1061/(ASCE)0733-9399(1999)125:1(26))
28. Sepahvand, K.: Stochastic finite element method for random harmonic analysis of composite plates with uncertain modal damping parameters. *J. Sound Vib.* **400**, 1–12 (2017). <https://doi.org/10.1016/j.jsv.2017.04.025>
29. Sepahvand, K.: Spectral stochastic finite element vibration analysis of fiber-reinforced composites with random fiber orientation. *Compos. Struct.* **145**, 119–128 (2016). <https://doi.org/10.1016/j.compstruct.2016.02.069>
30. Sasikumar, P., Suresh, R., Gupta, S.: Stochastic finite element analysis of layered composite beams with spatially varying non-Gaussian inhomogeneities. *Acta Mech.* 1503–1522 (2014). <https://doi.org/10.1007/s00707-013-1009-9>
31. Der Kiureghian, A., Ke, J.: The stochastic finite element method in structural reliability. *Probabilistic Eng. Mech.* **3**, 83–91 (1988). [https://doi.org/10.1016/0266-8920\(88\)90019-7](https://doi.org/10.1016/0266-8920(88)90019-7)
32. Vanmarcke, E., Grigoriu, M.: Stochastic Finite Element Analysis of Simple Beams. *J. Eng. Mech.* **109**, 1203–1214 (1983). [https://doi.org/10.1061/\(ASCE\)0733-9399\(1983\)109:5\(1203\)](https://doi.org/10.1061/(ASCE)0733-9399(1983)109:5(1203))
33. Chen, J., Li, J.: Optimal determination of frequencies in the spectral representation of stochastic processes. *Comput. Mech.* **51**, 791–806 (2013). <https://doi.org/10.1007/s00466-012-0764-0>
34. Zhang, J., Ellingwood, B.: Orthogonal Series Expansions of Random Fields in Reliability Analysis. *J. Eng. Mech.* **120**, 2660–2677 (1994). [https://doi.org/10.1061/\(ASCE\)0733-9399\(1994\)120:12\(2660\)](https://doi.org/10.1061/(ASCE)0733-9399(1994)120:12(2660))
35. Li, C., Der Kiureghian, A.: Optimal discretization of random fields. *J. Eng. Mech.-Asce.* **119**, 1136–1154 (1993). [https://doi.org/10.1061/\(ASCE\)0733-9399\(1993\)119:6\(1136\)](https://doi.org/10.1061/(ASCE)0733-9399(1993)119:6(1136))
36. Sudret, B., Der Kiureghian, A.: Stochastic finite element methods and reliability: a state-of-the-art report. Department of Civil and Environmental Engineering, University of California, Oakland (2000)
37. Rosenblueth, E.: Point estimates for probability moments. *Proc. Natl. Acad. Sci.* **72**, 3812–3814 (1975). <https://doi.org/10.1073/pnas.72.10.3812>

38. Seo, H.S., Kwak, B.M.: Efficient statistical tolerance analysis for general distributions using three-point information. *Int. J. Prod. Res.* **40**, 931–944 (2002). <https://doi.org/10.1080/00207540110095709>
39. Yan-Gang, Zhao, Tetsuro, Ono: New Point Estimates for Probability Moments. *J. Eng. Mech.* **126**, 433–436 (2000). [https://doi.org/10.1061/\(ASCE\)0733-9399\(2000\)126:4\(433\)](https://doi.org/10.1061/(ASCE)0733-9399(2000)126:4(433))
40. Zhou, J., Nowak, A.S.: Integration formulas to evaluate functions of random variables. *Struct. Saf.* **5**, 267–284 (1988). [https://doi.org/10.1016/0167-4730\(88\)90028-8](https://doi.org/10.1016/0167-4730(88)90028-8)
41. Fan, W., Wei, J., Ang, A.H.-S., Li, Z.: Adaptive estimation of statistical moments of the responses of random systems. *Probabilistic Eng. Mech.* **43**, 50–67 (2016). <https://doi.org/10.1016/j.probengmech.2015.10.005>
42. Liu, X., Xiang, P., Jiang, L., Lai, Z., Zhou, T., Chen, Y.: Stochastic Analysis of Train-bridge System Using the Karhunen–Loeve Expansion and the Point Estimate Method. *Int. J. Struct. Stab. Dyn.* (2019). <https://doi.org/10.1142/S021945542050025X>
43. Liu, X., Jiang, L., Lai, Z., Xiang, P., Chen, Y.: Sensitivity and dynamic analysis of train-bridge coupled system with multiple random factors. *Eng. Struct.* **221**, 111083 (2020). <https://doi.org/10.1016/j.engstruct.2020.111083>
44. Xu, H., Rahman, S.: A generalized dimension-reduction method for multidimensional integration in stochastic mechanics. *Int. J. Numer. Methods Eng.* **61**, 1992–2019 (2004). <https://doi.org/10.1002/nme.1135>
45. Zhao, Y., Lu, Z.: Cubic normal distribution and its significance in structural reliability. *Struct. Eng. Mech.* **28**, 263–280 (2008). <https://doi.org/10.12989/sem.2008.28.3.263>

**Publisher's Note** Springer Nature remains neutral with regard to jurisdictional claims in published maps and institutional affiliations.